CF$_2$H, a Hydrogen Bond Donor

Chanan D. Sessler[†], **Martin Rahm**[‡], **Sabine Becker**[†], **Jacob M. Goldberg**[†], **Fang Wang**[†], and **Stephen J. Lippard**[*,†]

[†]Department of Chemistry, Massachusetts Institute of Technology, 77 Massachusetts Avenue, Cambridge, MA 02139, United States

[‡]Department of Chemistry and Chemical Biology, Baker Laboratory, Cornell University, Ithaca, NY 14853, United States

Abstract

The CF$_2$H group, a potential surrogate for the OH group, can act as an unusual hydrogen bond donor, as confirmed by crystallographic, spectroscopic, and computational methods. Here, we demonstrate the bioisosterism of the OH and CF$_2$H groups and the important roles of CF$_2$–H···O hydrogen bonds in influencing intermolecular interactions and conformational preferences. Experimental evidence, corroborated by theory, reveals the distinctive nature of CF$_2$H hydrogen bonding interactions relative to their normal OH hydrogen bonding counterparts.

Graphical Abstract
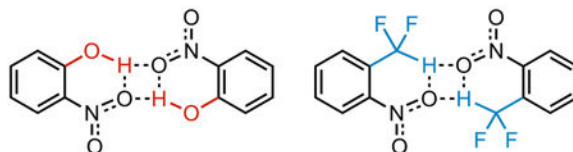
INTRODUCTION

Hydrogen bonding interactions play a crucial role in diverse chemical and biological processes, including catalysis,[1] protein folding, and maintaining the structure of the DNA double helix.[2-3] Strong hydrogen bond donors, such as O–H, N–H, and S–H functional groups, have been studied extensively.[2, 4] In contrast, the ability of C–H bonds to act as hydrogen bond donors did not receive much attention until relatively recently.[5-8] Although the difluoromethyl group (CF$_2$H) has long been proposed to act as a hydrogen bond donor and thus a surrogate for hydroxyl or thiol moieties, only a few experimental investigations have explored hydrogen bonding interactions of the CF$_2$H group in the condensed phase.[9-11] Here, we describe a thorough investigation of CF$_2$H hydrogen bonding interactions as revealed by NMR and IR spectroscopy, X-ray crystallography, and theoretical calculations.

Incorporation of fluorine can alter the properties of a compound, such as volatility,[12-14] conformational preference,[15-16] metabolic stability,[17-18] and acidity.[12] Difluorination of the methyl group leads to a significant increase in the acidity of the C–H bond,[19-21] presumably rendering the CF_2H group a better hydrogen bond donor than its non-fluorinated counterpart. Electrostatic potential surfaces reveal the high polarity of the CF_2H group (Table 1) compared to that of the methyl group and the possibility that CF_2H group is a hydrogen bond donor. As suggested by their σ_I values,[22] the CF_2H and OH groups have similar inductive properties. Based on its electronic characteristics and putative ability to act as a hydrogen bond donor, the CF_2H motif is considered a metabolically stable bioisostere of the OH group,[17] despite its greater steric bulk[23] and much weaker resonance effect (Table 1).[22]

The hydrogen bond donating ability of the CF_2H group has been proposed since the 1990s. Studies of simple CF_2H-containing molecules in the gas phase and in an argon matrix at 15 K support this claim,[9, 24-25] as do studies of hydrogen bonding interactions between CH_2F_2 and the extremely strong hydrogen bond acceptor F^-.[26] In addition, Erickson and McLoughlin investigated intramolecular hydrogen bonding between CF_2H and amide groups.[10] The hydrogen bonding ability of the CF_2H group was indirectly inferred from the red shifted carbonyl stretching frequency in solid state IR spectra, evidence that was corroborated by solution NMR spectroscopy and theoretical calculations. Smith and Scheiner studied the contribution of the intramolecular $CF_2-H \cdots O$ interaction to the conformational preference of an α,α-difluoroamide by X-ray crystallography and quantum mechanical calculations.[11] Short intramolecular $CF_2-H \cdots O/N$ distances have been observed in some X-ray structures and described as hydrogen bonding interactions.[27-28] We conducted a comprehensive survey of structures deposited in the Cambridge Crystal Structural Database and identified short $CF_2-H \cdots O$ distances (<2.7 Å) that may allow for hydrogen bonding interactions in 59 structures (See SI §6.1).

Recently, Zafrani et al. determined the hydrogen bond acidity of the CF_2H moiety based on ^{1}H NMR chemical shifts of the OCF_2H and SCF_2H protons.[29] These results suggest that CF_2H ethers and thioethers can act as hydrogen bond donors, but the influence of the neighboring oxygen or sulfur atoms on the hydrogen bonding ability of the CF_2H functional group may be considerable. Owing to the presence of α-oxygen and sulfur atoms, this work is presumably much more relevant to bioisosteres of the O–OH and S–OH moieties, which are less common functional groups than the C–OH group in medicinal chemistry and biology. Initial studies[9-11, 24] of $CF_2H \cdots X$ hydrogen bonding interactions have routinely been used to justify CF_2H functionalization of small molecules.[30-37] Several key questions regarding CF_2H hydrogen bonding interactions remain, including those concerning the relation between CF_2H and OH hydrogen bonding interactions, the nature of CF_2H hydrogen bonding, and the influence of CF_2H hydrogen bonding on the conformational behavior of molecules in solution. Studies of $CF_2-H \cdots O$ interactions have primarily been conducted in an intramolecular context, even though the influence of conformational preference can be better parsed intermolecularly. Surprisingly, such interactions are largely unexplored in the condensed phase.

RESULTS AND DISCUSSION

In the course of our research, we observed unusual ^{19}F NMR spin-spin coupling patterns in 2,2-difluoro-1-phenyl ethyl triflate derivatives in various solvents, features indicative of intramolecular CF_2H hydrogen bonding interactions. These observations prompted us to explore this phenomenon in simpler model compounds. We investigated intermolecular hydrogen bonding interactions in o-nitrophenol (**1-OH**, Fig. 1a) and o-nitro-α,α-difluorotoluene (**1-CF$_2$H**, Fig. 1b). Both **1-OH** and **1-CF$_2$H** crystallize in a similar manner as hydrogen-bonded dimers, suggesting bioisosterism of the CF_2H and OH groups (Figs. 1a-b). The intermolecular $CF_2–H\cdots O_2N$ bonding distance and $C–H\cdots O$ angle are 2.42(3) Å and 157(2)°, respectively, well in range of the sum of the van der Waals radii (~2.7 Å). In comparison, the corresponding $O–H\cdots O_2N$ distance and $O–H\cdots O$ angle in the **1-OH** dimer are 2.65(2) Å and 133(2)°.

X-ray structures indicate the presence of intramolecular $O/CF_2–H\cdots O_2N$ interactions in both **1-OH** and **1-CF$_2$H**. The intramolecular $O–H\cdots O_2N$ distance in **1-OH** (1.78(2) Å) is significantly shorter than the corresponding $CF_2–H\cdots O_2N$ distance in **1-CF$_2$H** (2.45(2) Å). The shorter $O–H\cdots O_2N$ distance, as well as the co-planarity of the nitro and hydroxyl groups, is facilitated by the smaller size of the hydroxyl group. In contrast, this arrangement is disfavored in **1-CF$_2$H** because of the greater steric bulk of the CF_2H group. The crystal packing of the **1-CF$_2$H** group requires approximately 0.14 Å more space than that observed in the **1-OH** stucture, which is consistent with the Charton parameters (see Table 1 and Figs. S44B and S45B).

Despite the structural similarity between **1-CF$_2$H** and **1-OH** in the crystalline state, IR spectroscopy reveals significant differences in the intramolecular OH and CF_2H hydrogen bonding interactions. To investigate the effect of hydrogen bonding on the O–H and CF_2–H bond stretching modes, we examined the IR spectra of compounds that cannot form intramolecular hydrogen bonds. We chose p-bromophenol (**2-OH**) and p-bromo-α,α-difluorotoluene (**2-CF$_2$H**) as reference compounds for **1-OH** and **1-CF$_2$H,** respectively (Figs. 1c-1d). The O–H stretching frequency of **1-OH** is red-shifted by -372 cm^{-1} relative to that of p-bromophenol (Fig. 1c). In contrast, the intramolecular $CF_2–H\cdots O_2N$ interaction in **1-CF$_2$H** leads to a $+44$ cm^{-1} blue shift in the CF_2–H stretch with decreased intensity relative to that in **2-CF$_2$H** (Fig. 1d). Decreased IR intensity is a characteristic of blue-shifting hydrogen bonds.[38] Our findings reveal that the $CF_2–H\cdots O_2N$ interaction is an example of a blue-shifting hydrogen bonding interaction, a known phenomenon.[39]

^1H NMR spectroscopy provides additional evidence for the presence of intramolecular $O/CF_2–H\cdots O_2N$ hydrogen bonding interactions. The CF_2H proton of **1-CF$_2$H** is significantly deshielded compared to that of **2-CF$_2$H** (δ = $+0.78$ ppm). This result is consistent with an electron density analysis (quantum theory of atoms in molecules, QTAIM) that showed the hydrogen bonded CF_2H proton of **I-CF$_2$H** to have $+0.04$ more positive charge than that of **2-CF$_2$H**. Moreover, deshielding of the CF_2H proton in deuterated chloroform is independent of **1-CF$_2$H** concentration over the range of 1 to 500 mM, a finding that indicates the presence of intramolecular hydrogen bonding interactions in **1-CF$_2$H** under these conditions. The concentration-independent deshielding of the hydroxyl proton of **1-OH** (δ

= +5.81 ppm compared to that of **2-OH)** also suggests the presence of intramolecular hydrogen bonding in **1-OH**, corresponding to an increase in the calculated atomic charge on the phenolic proton of **1-OH** by +0.07. Although the local diamagnetic contribution of the electron density around a proton is an important factor that affects the chemical shift, the influence of magnetic anisotropic effects of the nitro group can be non-negligible.[40]

We used density functional theory (DFT) to calculate the CF_2–$H \cdots O_2N$ and O–$H \cdots O_2N$ hydrogen bonding interactions in these systems. All structures and thermal corrections were evaluated at the M06-2X/6-31+G(d,p) level of theory in the gas phase (see SI §5.5.1). Final energies were obtained from M06-2X/aug-cc-pVTZ single-point calculations. Similar results were also obtained from calculations at the PCM(CHCl$_3$)-M06-2X/6-311++G(2d,2p)// PCM(CHCl$_3$)-B3LYP/6-31+G(d,p) level of theory (see SI §5.1.3.4—5.1.3.8). Monomeric **1-OH** has two conformers, **1-OH-a** and **1-OH-b** (Fig. 2a). Conformer **1-OH-a** has an intramolecular hydrogen bonding interaction and is predicted to be 9.9 kcal/mol lower in energy than the nonhydrogen bonding counterpart. In keeping with our observations in the crystalline state, the dimerization of **1-OH** is facilitated by two identical intermolecular hydrogen bonding interactions, adding up to 3.5 kcal/mol. In contrast, three conformers were identified for monomeric **1-CF$_2$H** (Figs. 2b and S38). In **1-CF$_2$H-a**, intramolecular hydrogen bonding interactions appear to be present and this conformer is 4.3 kcal/mol lower in energy compared to the non-hydrogen bonding **1-CF$_2$H-b.** Steric effects are a significant driving force behind this energy difference and, as discussed below, the stabilization of **1-CF$_2$H-a** cannot be solely attributed to a bonding interaction.

Intermolecular CF_2–$H \cdots O_2N$ interactions also lead to dimerization of **1-CF$_2$H-a** to form (**1-CF$_2$H-a**)$_2$. The structure of the dimer observed in the crystalline state is similar to that predicted by DFT calculation in the gas phase (Fig. 1b). The dimerization of **1-CF$_2$H** structurally and energetically resembles that of **1-OH**. Both dimerization processes provide ca 3.1 kcal/mol stabilization (Fig. 2, Table 2). Our calculations predict the CF_2–H stretching frequency of **1-CF$_2$H-a** to be blue-shifted by ca. +72 cm^{-1} (unscaled) relative to that of **1-CF$_2$H-b**. Because the IR spectrum of **1-CF$_2$H** has contributions from both **1-CF$_2$H-a** and **1-CF$_2$H-b**, an experimental determination of the relative IR shift is challenging. To better validate our theoretical calculations, we compared the computed CF_2–H stretching frequency in **1-CF$_2$H-a** to that in **2-CF$_2$H**. The former is blue shifted by ca. +81 cm^{-1} (unscaled; Scheme S2). This result is qualitatively consistent with the experimental observation of a shift of +44 cm^{-1} between **1-CF$_2$H** and **2-CF$_2$H** (Fig. 1d) and the blue-shifting nature of the CF$_2$H hydrogen bonding interaction. Dimerization of **1-CF$_2$H-a** to form (**1-CF$_2$H-a**)$_2$ results in a further blue shift of +11 cm^{-1}. In contrast, we calculated that **1-OH-a** should be red shifted by –287 cm^{-1} (unscaled) relative to **2-OH**. This result resembles the experimental value of –372 cm^{-1}.

With these results in hand, we explored by NMR spectroscopy the influence of CF$_2$H hydrogen bonding interactions on the properties and conformational behavior of a more complicated molecule, 2,2-difluoro-1-(2-nitrophenyl)ethyl triflate (**4-NO$_2$**). This compound has more rotational freedom than **1-CF$_2$H**. As shown in Scheme 1, we prepared **3-NO$_2$** by

treating the corresponding aldehyde with $TMSCF_2H$.[41-42] Triflation of **3-NO$_2$** afforded **4-NO$_2$**.

As depicted in Figs. 3a-b, **4-NO$_2$** exhibits unusual NMR features. The trifluoromethyl (CF_3) group, generally a singlet in the ^{19}F NMR spectrum, unexpectedly appears as a doublet (δ = −74.3 ppm, J = 4.1 Hz) in the spectrum of **4-NO$_2$** in $CDCl_3$ (Fig. 3b-e). F^a exhibits the expected doublet of doublets of doublets (δ = −133.7 ppm, ddd, $^2J_{Fa-Fb}$ = 285.5 Hz, $^2J_{Fa-H1}$ = 53.8 Hz, $^3J_{Fa-H2}$ = 15.6 Hz, Fig. 3e), but F^b is a doublet of doublets of doublets of quartets (δ = −124.5 ppm, dddq, $^2J_{Fb-Fa}$ = 285.7 Hz, $^2J_{Fb-H1}$ = 53.7 Hz, $^3J_{Fb-H2}$ = 5.6 Hz, $J_{Fb-CF3, through space}$ = 4.1 Hz , Figs. 3c-d). These quartets of 4.1 Hz, most likely the consequence of through-space ^{19}F-^{19}F coupling with the CF_3 group of the triflate, suggest that **4-NO$_2$** adopts a conformation in which F^b is spatially close to the CF_3 group.[43] Moreover, the through-space ^{19}F-^{19}F coupling constant is essentially independent of solvents and concentration, indicating the high conformational rigidity of **4-NO$_2$** (Figs. S2 and S3). The ^1H NMR spectrum of **4-NO$_2$** in $CDCl_3$ shows a vicinal coupling constant $^3J_{H1-H2}$ of 1.7 Hz. According to a modified Karplus equation that accounts for substituent effects,[44] this value corresponds to an H1-C1-C2-H2 dihedral angle of 68° or 43°. In addition to 1D NMR studies, the ^1H-^{19}F 2D heteronuclear NOESY (HOESY) spectrum of **4-NO$_2$** displays a strong NOE between H1 and the CF_3 group but a weak H6-F^a interaction. From these results we conclude that the CF_2–H bond of **4-NO$_2$** points toward the NO_2 moiety, possibly facilitating an intramolecular hydrogen bonding interaction (Fig. 3a).

We also prepared 2,2-difluoro-1-(4-bromophenyl)ethyl triflate (**4-Br**, Fig. 3f) and 2,2-difluoro-1-(2-fluorophenyl)ethyl triflate (**4-F**, Fig. 3k), neither of which should exhibit significant intramolecular hydrogen bonding interactions. As in **1-CF$_2$H**, we found that the CF_2H proton of **4-NO$_2$** shifts down-field by 0.27 ppm and 0.13 ppm relative to those of **4-Br** and **4-F**, respectively, a result suggesting the presence of intramolecular hydrogen bonding interactions in **4-NO$_2$**.

Conformational analysis suggests that **4-Br** and **4-F** behave differently than **4-NO$_2$**. Unlike that of **4-NO$_2$**, the ^{19}F NMR signal of the CF_3 group of **4-Br** is a pseudo triplet owing to through-space coupling with F^a and F^b of 2.4 Hz and 1.1 Hz, respectively (Fig. 3g). Presumably, the slightly stronger coupling of the CF_3 group with F^a indicates that F^a is closer than F^b is to the CF_3 group (Fig. 3f). Analysis of the coupling constants of H2 further supports this hypothesis. The $^3J_{H1-H2}$ of 4.1 Hz indicates a nearly antiparallel geometry for the H1-C1-C2-H2 unit (147°) based on a modified Karplus equation.[44] The values of $^3J_{H2-Fa}$ and $^3J_{H2-Fb}$ (ca. 10 Hz) suggest similar F^a-C1-C2-H2 and F^b-C1-C2-H2 dihedral angles, an observation that supports the proposed H1-C1-C2-H2 arrangement (Figs. 3h-j). Taken together, these results suggest that the orientation of the CF_2H group of **4-Br** differs from that of **4-NO$_2$**, most likely due to CF_2–H···O_2N hydrogen bonding.

The CF_3 group of **4-F** is spatially close to both F^a and F^b, as indicated by the through-space coupling of 1.8 Hz with F^a and F^b (Fig. 3l). The multiplicity of the benzylic proton of **4-F** is similar to that of **4-Br**, particularly the $^3J_{H1-H2}$ of 4.2 Hz, and corresponds to that of a nearly identical H1-C1-C2-H2 dihedral angle. A through-space coupling analysis of the aromatic fluorine atom, F^d, provides additional structural information. As shown in the $^{19}F\{^1H\}$

NMR spectrum the through-space coupling constants of F^d with F^a and F^b are identical ($J_{\text{through-space}}$ = 3.0 Hz), indicating possibly similar $F^d \cdots F^a$ and $F^d \cdots F^b$ distances (Fig. 3m). This analysis suggests a dominant *"anti"* arrangement of the CF_2–H bond with respect to the C8–F^d bond, which is consistent with the rather weak through-space coupling between F^d and H1 (0.8 Hz) observed in the ^{1}H NMR spectrum (Fig. S100). This conformational analysis demonstrates that **4-F** has a 3D geometry similar to that of **4-Br**. Taken together, these results indicate that the presence of a relatively strong hydrogen bond acceptor, such as a nitro group, can alter the conformational preference of the CF_2–H bond. By comparison, very weak hydrogen bond acceptors, such as the C–F motif,[45] have little influence on the orientation of CF_2–H bonds. Moreover, the proton of the CF_2H group is deshielded in **4-NO$_2$** (δ = 6.25 ppm) compared to those in **4-F** (δ = 6.12 ppm) and **4-Br** (δ = 5.98 ppm), a trend indicating the presence of a relatively strong hydrogen bonding interaction in **4-NO$_2$**. As discussed in the supporting information (§8), a similar trend can be seen in a series of *ortho*- substituted α-difluoromethylbenzyl alcohols (ArCH(OH)CF$_2$H) in which greater deshielding of the CF_2H proton is associated with stronger hydrogen bond acceptors in the *ortho* position.

We also investigated the vibrational properties of the CF_2H group in the three model compounds, **4-NO$_2$**, **4-Br**, and **4-F**. As discussed above, **4-Br** and **4-F** are reference compounds that do not exhibit significant hydrogen bonding interactions. We identified the CF_2–H bond stretching frequencies of **4-NO$_2$** and **4-Br** by comparing their IR spectra to those of the corresponding CF_2D-containing analogues, **4-NO$_2$-D** and **4-Br-D**. The stretching frequency of the **4-Br** CF_2–H bond occurs at 2972 cm^{-1} (Figs. S8C-D). Even though **4-F** allows for the F^d atom to be in close proximity to the H1 atom in several populated conformations, the **4-F** CF_2–H bond stretching frequency is almost identical (2971 cm^{-1}; Fig. S10). The CF_2–H region of the IR spectrum of **4-NO$_2$** is complicated, but we tentatively assigned the peak at 3008 cm^{-1} to the CF_2–H stretch, corresponding to a blue shift of +36 cm^{-1} relative to **4-Br** (Fig. S6). This result is consistent with the blue-shifting nature of the $CF_2H \cdots O_2N$ interaction in **1-CF$_2$H**, which is blue shifted by +44 cm^{-1} relative to that of **2-CF$_2$H**.

We used DFT calculations to explore the conformational distribution of **4-NO$_2$**, **4-Br**, and **4-F** (Fig. S18, S20, and S22). Our theoretical calculations suggest that the H1-C1-C2-H2 unit of the preferred **4-NO$_2$** conformer adopts a *gauche* arrangement due to intramolecular CF_2–H$\cdots O_2N$ interactions, as shown in Fig. 3a. The CF_2–H$\cdots O_2N$ distances are ~2.5 Å. In contrast, the non-hydrogen bonding model compounds **4-Br** and **4-F** prefer an *anti* H1-C1-C2-H2 geometry, as shown in Figs. 3f and 3k. These theoretical results are in good agreement with the results of our NMR conformational analysis. To verify the calculated conformational distributions for each molecule, we predicted the ^{1}H, ^{19}F, and ^{13}C NMR chemical shifts of the major conformers of **4-NO$_2$, 4-Br**, and **4-F** at the GIAO-PCM-B3LYP/aug-cc-pVTZ level. The population-weighted predicted chemical shifts agree well with the experimental values, suggesting that the conformational distribution is well described by the theoretical model (SI §5.2). The calculated IR stretching frequencies of the CF_2–H bond are within 12 cm^{-1} (scaled) of the experimental values, confirming the blue-shifting nature of the CF_2–H$\cdots O_2N$ interactions. Our analysis of **4-NO$_2$** and **4-Br** indicates

that the CF_2–H$\cdots O_2$N hydrogen bonding interaction is sufficiently strong to alter the conformational preference of more complicated molecules in solution.

A variety of explanations for blue-shifting hydrogen bonds have been suggested in the literature.[38, 46-50] One rationalization for blue-shifting hydrogen bonding interactions invokes electronegativity equalization as embodied in Bent's rule.[48,51] In this model, the approaching hydrogen bond acceptor induces a polarization of the donor bond ($X^{\delta-}$–$H^{\delta+}\cdots A^{\delta-}$). The increased negative charge on the donor atom (X) corresponds to an increased electronegativity, which in turn is made possible by an increased s-character of X. Increased s-character leads to a shorter bond and a blue shift of the X–H stretching vibration. This blue-shifting effect can also be expressed in terms of electron donation from the hydrogen bond acceptor into the hydrogen bond donor (X–H bond), which is strengthened.[9, 38] The bond lengthening and red shifting of 'normal' hydrogen bonding interactions can, in contrast, be explained by the more predominant effect of electron donation into the C–H σ^* orbital, through hyperconjugation.[38, 48]

The existence of these two competing processes allows for charge transfer to the hydrogen bond acceptor, in different manners. We performed topological analyses of the calculated electron densities before and after hydrogen bonding in our examples of red- and blue-shifting hydrogen bonding interactions. These results indicate that between 0.01 and 0.08 electrons are transferred to the hydrogen bond donor in either case (see Table S2).

An appealing justification for blue shifting, as discussed above, invokes electronegativity, or more precicely, the change in electronegativity upon bond formation. To quantify the degree of 'electronegativity equalization' associated with the processes of forming hydrogen bonding interactions, we employed an energy partitioning analysis that defines electronegativity as the average binding energy, $\bar{\chi}$.[52-53] In this framework, the reaction or bond energy, E, can be expressed as the sum of three terms,

$$\Delta E \, / \, n = \Delta\bar{\chi} + \Delta(V_{NN} + \omega) \, / \, n, \quad \text{(Eq.1)}$$

where n is the number of electrons, V_{NN} is the change in nuclear-nuclear repulsion due to structural transformation over a reaction, and ω encompasses all ways that electrons, on average, change their interactions over the course of a reaction. The quantity $\bar{\chi}$ is a measure of how strongly the average electron is bound to a system. Similarly, $\Delta\bar{\chi}$ captures the change in overall electronegativity over a given transformation, i.e., it expresses electronegativity equalization. Another way of interpreting $\Delta\bar{\chi}$ is as the average orbital stabilization, which in turn is related to the degree of covalency.[53]

As we attempt to rationalize and analyze these bonding processes it is important to keep in mind that a) the interactions are weak, <4 kcal/mol, and b) a shift of a vibrational frequency of ca. 40 cm^{-1} corresponds to a change in energy of only ~0.1 kcal/mol—a small value in comparison to the classical Pauling unit (PU) of electronegativity, which can be translated into energy as 1 PU ≈ 140 kcal/mol (see SI §5.5.1).

The data in Table 2 illustrate that the rotation of a hydrogen bond donating group in both **1-OH** and **1-CF$_2$H**, which leads to red and blue shifts of the O–H and C–H stretching vibrations, respectively, corresponds to a *decrease* in $\bar{\chi}$. When $\Delta\bar{\chi} < 0$, both processes are favored by orbital stabilization, indicating that a degree of covalency is at play. One marked difference between the two intramolecular processes becomes apparent when considering V_{NN}/n. This term is in a sense an overall measure of the change in steric crowding during a structural change. The blue-shifting **1-CF$_2$H-b $\rightarrow$ 1-CF$_2$H-a** process corresponds to an overall *relaxation* of nuclear-nuclear repulsion, whereas, in the red-shifting **1-OH-b $\rightarrow$ 1-OH-a** event, nuclei move on average closer together. The latter is a clear indication of bonding in a delocalized sense, whereas the former may be interpreted as being driven by both the release of steric crowding in addition to a favorable orbital interaction.

These two intramolecular transformations exemplify a fundamental challenge with analyzing such processes, namely, our inability to uniquely separate the reaction energy into parts attributable to local bonding interactions and all other aspects of the structural rearrangement in question. In order to parse out the underlying cause-and-effect in hydrogen bonding we also considered intermolecular interactions. In energetically favorable dimerization processes, the net structural change is always due to favorable intermolecular bonding interactions.

All intermolecular hydrogen bonding processes shown in Table 2 are characterized by *increases* in $\bar{\chi}$ ($\Delta\bar{\chi} > 0$). On average, these bonds are all *disfavored* by the destabilization of orbitals. Alternatively, they are all characterized by an overall net *decrease* in electronegativity as the bond forms. This somewhat counterintuitive bonding situation is, in fact, common and characteristic of polar, ionic, and metallogenic bonds, and of charge transfer processes.[53] For bonding processes where $\Delta\bar{\chi} > 0$, the energy lowering associated with bond formation arises solely from the introduction of multielectron interactions, ω (Eq 1). As already discussed, a degree of charge transfer is an expected prerequisite of both red- and blue-shifting hydrogen bonding interactions (Table S2).

To differentiate red- from blue-shifting intermolecular hydrogen bonding interactions we turn to a bonding descriptor that is reflective of the energy partitioning shown as Eq 1, and that has also shown property-predictive promise,[53]

$$Q = (\Delta\bar{\chi} - \Delta(V_{NN} + \omega)\,/\,n)\,/\,\Delta E = 2n\Delta\bar{\chi}\,/\,\Delta E - 1 \quad \text{(Eq.2)}$$

Q quantifies the balance between the $\Delta\bar{\chi}$ (electronegativity equalization and orbital stabilization) term and the $(V_{NN}+\omega)/n$ term, which quantifies charge-drift due to bonding interactions. On the positive side of the scale, Q ranges from Q=1, attributed to 'perfect covalency,' to Q>1, where disfavoring electron-electron interactions become more significant, to Q>>1, where dispersion and strong electrostatic interactions fall. On the negative side, Q=−1 is associated with 'perfect ionicity' and Q<−1 corresponds to polar, ionic and metallogenic bonds, where electron-electron interactions play an increasingly important role. Examples of Q for a representative range of bonding interactions are Xe$_2$ (~60 "dispersion, highly correlated"), F$_2$ (16, "covalent, highly correlated"), CO (4,

"covalent"), HF (−2, "polar"), NaH (−7, "ionic"), Na_2 (−35, "metallogenic") and CsI (−100, "ionic, highly correlated"). The bond energy represents a natural second dimension of what is a veritable map of bonding interactions.[53]

All intramolecular hydrogen bonding interactions are characterized by negative values of Q, a result supporting the interpretation of charge transfer as being concurrent with these processes. "Normal" red-shifting hydrogen bonding interactions, here exemplified by water dimerization, **2-OH** + DMF complexation, and guanine-cytosine base pairing, correspond to more moderate Q values of −6, −32 and −35, respectively. The blue-shifting interactions considered are distinctly different, and associated with substantially negative Q values, < −200. A very large absolute value of Q does not necessitate a small ΔE. Rather it means that the two terms adding up to the bond energy in Eq 1, i.e. $\Delta \bar{\chi}$ and $(V_{NN} + \omega)/n$, are of opposite sign but of nearly equal magnitude (Eq 2). This unusual situation of near equal-opposite terms will generate a Q value that is large and increasingly sensitive to the level of theory (or the experimental accuracy). Regardless of the exact value of Q, intermolecular blue-shifting hydrogen bonding interactions inhabit a distinct region on this scale of chemical interactions. The region of blue-shifting hydrogen bonding interactions is, in a manner of speaking, the antithesis of attractive electrostatic interactions. The strong formation of the NaCl dimer from *prepolarized* Na^+ and Cl^- ions corresponds to Q = +60 and +350 in the gas phase and in aqueous solution, respectively.[53] In recent work on blue-shifting hydrogen bonds using a Block-Localized Wavefunction Energy Decomposition approach,[46] the electron-electron electrostatic repulsion term is identified as the dominant driving force behind the blue shifting phenomenon. In our approach, changes to electron-electron electrostatic repulsion are included in the ω term (Eq. 1). Assuming that exchange and correlation effects, which are more short range, are less important, for $\omega > 0$, the electron-electron electrostatic repulsion must decrease over the hydrogen bond forming reaction.[52-53]

CONCLUSION

In conclusion, our experimental and theoretical studies support the long-proposed hydrogen bond donor ability of the CF_2H moiety.[9-11] Structural, spectroscopic, and computational comparisons between *o*-nitrophenol and *o*-nitro-α,α-difluorotoluene confirmed the bioisosterism of the CF_2H and OH functional groups. In particular, IR spectroscopy revealed the blue-shifting nature of CF_2H hydrogen bonding interactions in solution. We utilized a recently developed method for energy partitioning to quantify the chemical notion of electronegativity equalization in the different bonding processes and to highlight subtle differences in the electronic structure between them. Using a variety of techniques, we found that CF_2H hydrogen bonding interactions provide sufficient stabilization to facilitate the dimerization as well as to influence the conformational preference of CF_2H-containing molecules. The moderate strength of CF_2H interactions can, in principle, be exploited to design molecules that disrupt other hydrogen bonding interactions encountered in chemical biology and pharmaceutical science. These findings validate the use of the CF_2H group as a functional OH surrogate in chemical and medicinal applications and offer insight into the nature of CF_2H hydrogen bonding interactions.

Supplementary Material

Refer to Web version on PubMed Central for supplementary material.

REFERENCES

1. Doyle AG; Jacobsen EN, Chem. Rev. 2007, 107, 5713–5743. [PubMed: 18072808]

2. Jeffrey GA; Saenger W, The Importance of Hydrogen Bonds. Springer-Verlag: Berlin, Heidelberg, 1991; p 3–14.

3. Anslyn EV; Dougherty DA, Modern Physical Organic Chemistry. University Science: Sausalito, CA, 2006.

4. Pauling L, J. Am. Chem. Soc. 1931, 53, 1367–1400.

5. Desiraju GR; Steiner T, The Weak Hydrogen Bond in Structural Chemistry and Biology. Oxford University Press: Oxford, 1999; Vol. 9, p 507.

6. Derewenda ZS; Lee L; Derewenda U, J. Mol. Biol. 1995, 252, 248–262. [PubMed: 7674305]

7. Scheiner S, Phys. Chem. Chem. Phys. 2011, 13, 13860–13872. [PubMed: 21573303]

8. Yoon D-W; Gross DE; Lynch VM; Sessler JL; Hay BP; Lee C-H, Angew. Chem. Int. Ed. 2008, 47, 5038–5042.

9. Caminati W; Melandri S; Moreschini P; Favero PG, Angew. Chem. Int. Ed. 1999, 38, 2924–2925.

10. Erickson JA; McLoughlin JI, J. Org. Chem. 1995, 60, 1626–1631.

11. Jones CR; Baruah PK; Thompson AL; Schemer S; Smith MD, J. Am. Chem. Soc. 2012, 134, 12064–12071. [PubMed: 22789294]

12. Kirsch P, Introduction In Modern Fluoroorganic Chemistry, Wiley-VCH Verlag GmbH & Co. KGaA: 2013.

13. Bajzer WX, Fluorine Compounds, Organic In Kirk-Othmer Encyclopedia of Chemical Technology, John Wiley & Sons, Inc.: 2000.

14. Lippard SJ, J. Am. Chem. Soc. 1966, 88, 4300–4301.

15. Zimmer LE; Sparr C; Gilmour R, Angew. Chem. Int. Ed. 2011, 50, 11860–11871.

16. O'Hagan D, Chem. Soc. Rev. 2008, 37, 308–319. [PubMed: 18197347]

17. Bégué J-P; Bonnet-Delpon D, Effects of Fluorine Substitution on Biological Properties. John Wiley & Sons, Inc.: 2007; p 72–98.

18. Wang J; Sánchez-Roselló M; Aceña JL; del Pozo C; Sorochinsky AE; Fustero S; Soloshonok VA; Liu H, Chem. Rev. 2014, 114, 2432–2506. [PubMed: 24299176]

19. Streitwieser A Jr.; Mares F, J. Am. Chem. Soc. 1968, 90, 2444–2445.

20. Bordwell FG; McCallum RJ; Olmstead WN, J. Org. Chem. 1984, 49, 1424–1427.

21. Bordwell FG; Algrim D; Vanier NR, J. Org. Chem. 1977, 42, 1817–1819.

22. Hansch C; Leo A; Taft RW, Chem. Rev. 1991, 91, 165–195.

23. Charton M, The Prediction of Chemical Lability through Substituent Effects In Design of Biopharmaceutical Properties through Prodrugs and Analogs, Roche EB, Ed. American Pharmaceutical Association: Washington, DC, 1977; pp 228–280.

24. Feng G; Evangelisti L; Cacelli I; Carbonaro L; Prampolini G ; Caminati W, Chem. Commun. 2014, 50, 171–173.

25. Jeng M-LH; Ault BS, J. Mol. Struct. 1991, 246, 33–44.

26. Mahjoub AR; Zhang X; Seppelt K, Chem. Eur. J. 1995, 1, 261–265.

27. Prakash GKS; Krishnamoorthy S; Ganesh SK; Kulkarni A ; Haiges R; Olah GA, Org. Lett. 2014, 16, 54–57. [PubMed: 24295125]

28. Mironov VF; Zagidullina ER; Ivkova GA; Dobrynin AB; Gubaidullin AT; Latypov SK; Musin RZ; Litvinov IA; Balandina AA; Konovalova IV, Arkivoc 2004, 95–127.

29. Zafrani Y; Yeffet D; Sod-Moriah G; Berliner A; Amir D; Marciano D; Gershonov E; Saphier S, J. Med. Chem. 2017, 60, 797–804. [PubMed: 28051859]

30. Narjes F; Koehler KF; Koch U; Gerlach B; Colarusso S; SteinMhler C; Brunetti M; Altamura S; De Francesco R; Matassa VG, Bioorg. Med. Chem. Lett. 2002, 12, 701–704. [PubMed: 11844705]

31. Asante V; Mortier J; Wolber G; Koksch B, Amino Acids 2014 46, 2733–2744. [PubMed: 25193166]

32. Ni C; Hu M; Hu J, Chem. Rev. 2015, 115, 765–825. [PubMed: 25144886]

33. Prakash GKS; Hu J, Acc. Chem. Res. 2007, 40, 921–930. [PubMed: 17708659]

34. Camerino E; Wong DM; Tong F; Körber F; Gross AD; Islam R; Viayna E; Mutunga JM; Li J; Totrov MM; Bloomquist JR; Carlier PR, Bioorg. Med. Chem. Lett. 2014, 25, 4405–4411.

35. Hartz RA; Ahuja VT; Rafalski M; Schmitz WD; Brenner AB; Denhart DJ; Ditta JL; Deskus JA; Yue EW; Arvanitis AG; Lelas S; Li Y-W; Molski TF; Wong G ; Grace JE; Lentz KA; Li J; Lodge NJ; Zaczek R; Combs AP; Olson RE; Mattson RJ; Bronson JJ; Macor JE, J. Med. Chem. 2009, 52, 4161–4172. [PubMed: 19552436]

36. Thompson S; McMahon SA; Naismith JH; O'Hagan D, Bioorg. Chem. 2016, 64, 37–41. [PubMed: 26642178]

37. Prakash GKS; Mandal M; Schweizer S; Petasis NA; Olah GA, J. Org. Chem. 2002, 67, 3718–3723. [PubMed: 12027685]

38. Joseph J; Jemmis ED, J. Am. Chem. Soc. 2007, 129, 4620–4632. [PubMed: 17375920]

39. Hobza P; Havlas Z, Chem. Rev. 2000, 100, 4253–4264. [PubMed: 11749346]

40. Günther H, NMR Spectroscopy: Basic Principles, Concepts and Applications in Chemistry. 2nd **ed.;** John Wiley & Sons: Chichester, 1995.**ed.;**

41. Zhao Y; Huang W; Zheng J; Hu J, Org. Lett. 2011, 13, 5342–5345. [PubMed: 21910464]

42. Tyutyunov AA; Boyko VE; Igoumnov SM The Unusual Reaction of (Trifluoromethyl)Trimethylsilane with Sodium Borohydride *Fluorine Notes* [Online], 2011 http://notes.fluorine1.ru/public/2011/1_2011/letters/letter2.html (accessed Mar 3, 2017).

43. Dolbier WR Jr., An Overview of Fluorine NMR. John Wiley & Sons, Inc.: 2016; p 9–53.

44. Haasnoot CAG; de Leeuw FAAM; Altona C, Tetrahedron 1980, 36, 2783–2792.

45. Dunitz JD; Taylor R, Chem. Eur. J. 1997, 3, 89–98.

46. Wang C; Danovich D; Shaik S; Mo Y, J. Chem. Theory Comput. 2017, 13, 1626–1637. [PubMed: 28252964]

47. Hobza P; Špirko V. r.; Havlas Z; Buchhold K; Reimann B; Barth H-D; Brutschy B, Chem. Phys. Lett. 1999, 299, 180–186.

48. Alabugin IV; Manoharan M; Peabody S; Weinhold F, J. Am. Chem. Soc. 2003, 125, 5973–5987. [PubMed: 12733938]

49. Li X; Liu L; Schlegel HB, J. Am. Chem. Soc. 2002, 124, 9639–9647. [PubMed: 12167060]

50. Mo Y; Wang C; Guan L; Braïda B; Hiberty PC; Wu W, Chem. Eur. J. 2014, 20, 8444–8452. [PubMed: 24862363]

51. Bent HA, Chem. Rev. 1961, 61, 275–311.

52. Rahm M; Hoffmann R, J. Am. Chem. Soc. 2015, 137, 10282–10291. [PubMed: 26193123]

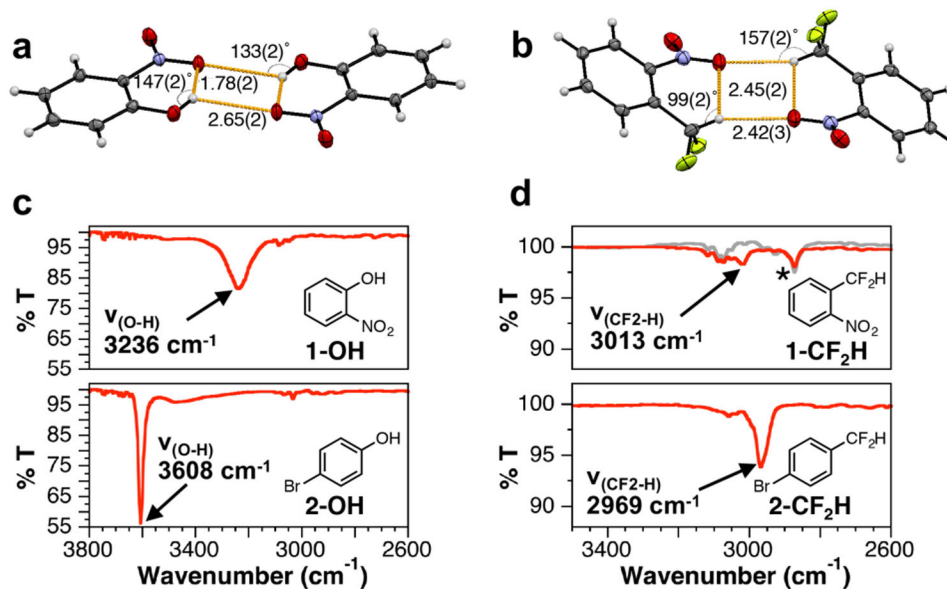53. Rahm M; Hoffmann R, J. Am. Chem. Soc. 2016, 138, 3731–3744. [PubMed: 26910496]

Figure 1.
(a, b) Crystal structures of **1-OH** and **I-CF₂H**; (c, d) IR spectra of 100 mM of **1-OH**, *p*-bromophenol (**2-OH**), **1-CF₂H**, and *p*-bromo-α,α-difluorotoluene (**2-CF₂H**) in CCl₄. Red and grey traces in panel (d) correspond to CF₂H- and CF₂D-containing compounds, respectively. Peaks of interest are identified with arrows. In panel d, the peak labeled with the asterisk appears in the IR spectra of both **1-CF₂H** and **1-CF₂D**, suggesting that it cannot be attributed to a CF₂–H stretching mode. The O–H stretching of **1-OH** is red shifted by -372 cm^{-1} relative to that of **2-OH**. In contrast, the CF₂–H stretching of **1-CF₂H** is blue shifted by $+44$ cm^{-1} relative to that of **2-CF₂H**.
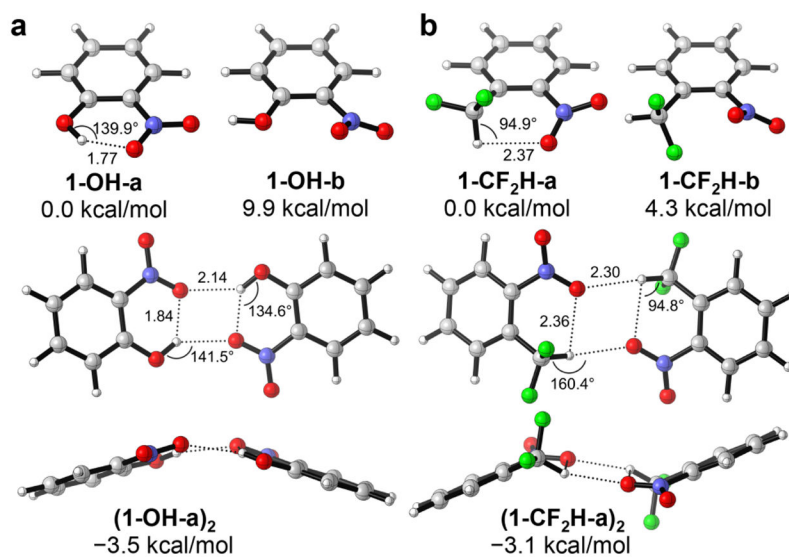
Figure 2.
Selected conformations/dimers of *o*-nitrophenol (a; **1-OH**) and *o*-nitro-α,α-difluorotoluene (b; **I-CF₂H**) in the gas phase and calculated relative energies (*E*). ¹H NMR spectroscopic studies showed **1-OH** and **1-CF₂H** to be predominantly monomeric in 100 mM CDCl₃ solutions.
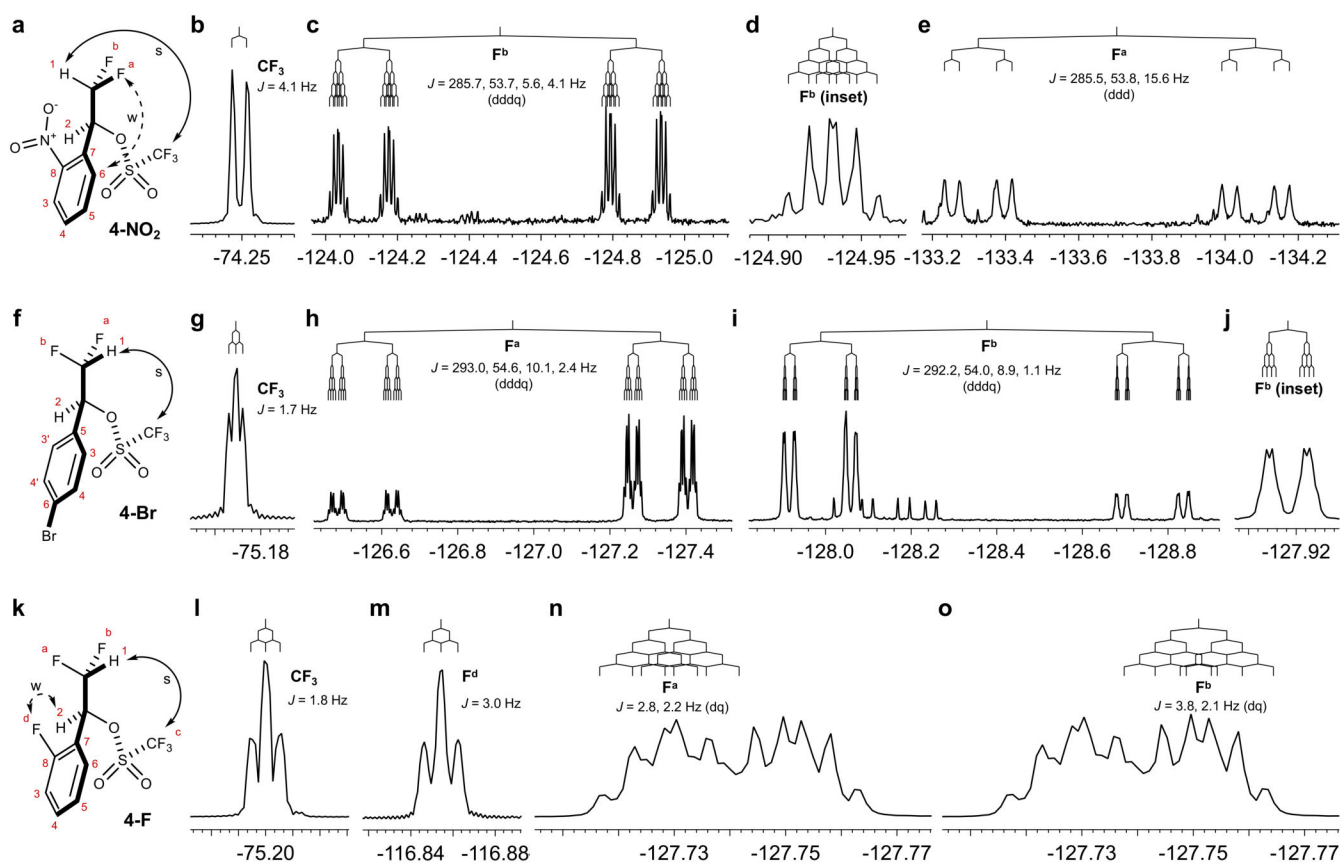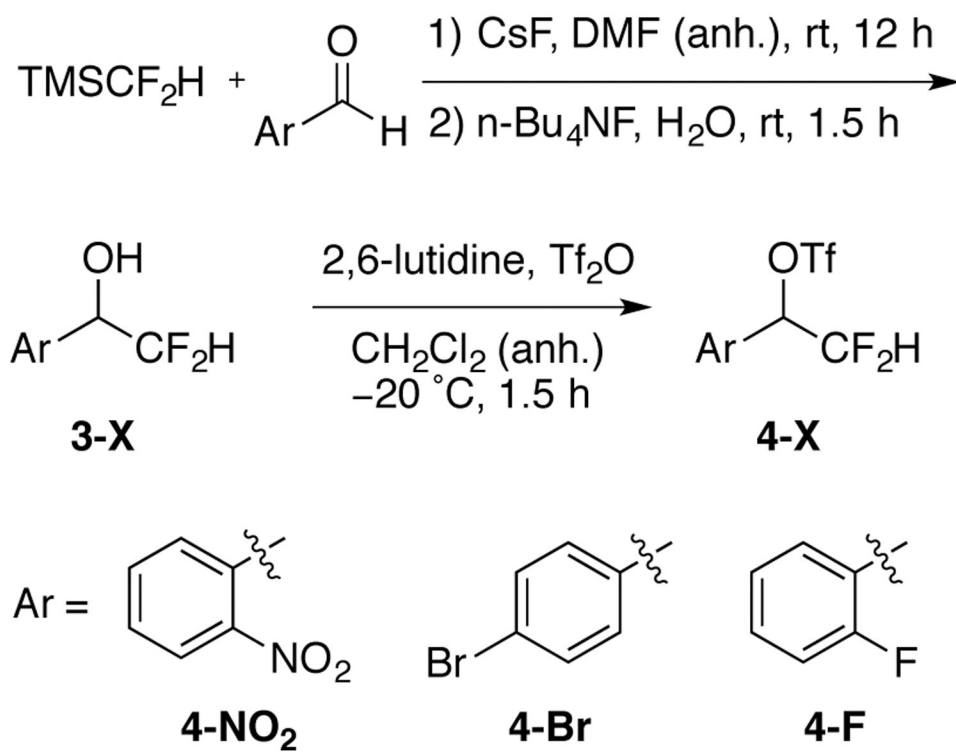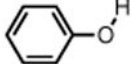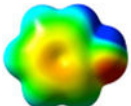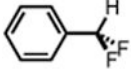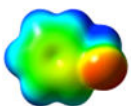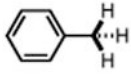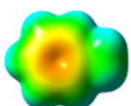
Figure 3.
NMR conformational analysis of **4-NO$_2$** (a), **4-Br** (f), and **4-F** (k) in CDCl$_3$ at a concentration of 50 mM. Strong (s) and weak (w) NOE interactions observed in ^{1}H-^{19}F HOESY are depicted with solid and dashed double-headed arrows, respectively. Coupling constant analyses of F^b and F^a are shown for each molecule (b-e, g-j, and l-o). Panels l-o are from the ^{19}F{^{1}H} NMR spectrum of **4-F**.

Scheme 1.
Synthesis of 2,2-difluoro-1-phenyl ethyl triflate derivatives (4-X) from 2,2-difluoro-1-phenyl ethan-1-ol (3-X).

Table 1.

Comparison of OH, CF_2H, and CH_3 Group Properties

Ph-X, Dipole moment (Debye)	Electrostatic potential surface[a]	σ_R[b]	σ_I[b]	Charton steric parameter (v)[c]	Acidity (pKa in DMSO)
1.693		−0.70	0.33	0.32	18.0[d]
3.277		0.03	0.29	0.68	Kinetic acidity ~10⁴ higher than PhMe[e]
0.523		−0.18	0.01	0.52	42[f]

[a] The electrostatic potential plotted on an isodensity surface of the electron density set to 0.001 e/bohr³. Red = −25 kcal/mol, blue = +25 kcal/mol.

[b] σ_R and σ_I are resonance and inductive effect parameters, respectively. Reference 22.

[c] Reference 23.

[d] Reference 21.

[e] Reference 19.

[f] Reference 20.

Table 2.

Energy partitioning analysis of selected interactions.

	E^a (kcal/mol)	$\Delta\bar{\chi}$ (kcal/mol)	V_{NN}/n (kcal/mol)	$(V_{NN}+\omega)/n$ (kcal/mol)	Q^b	X–H shift^c (cm^{-1})
Intramolecular:						
1-OH-b → **1-OH-a**	−9.9	−3.69	15.4	3.55	53	−250 (red)
1-CF$_2$H-b → **1-CF$_2$H-a**	−4.3	−0.99	−37.0	0.95	40	+72 (blue)
Intermolecular:						
2 **1-OH-a** → (**1-OH-a**)$_2$	−3.5	2.99	1967.1	−3.02	−250	+70 (blue)
2 **1-CF$_2$H-a** → (**1-CF$_2$H-a**)$_2$	−3.1	3.64	2328.7	−3.66	−420	+11 (blue)
2 CH$_2$F$_2$ → (CH$_2$F$_2$)$_2$	−1.7	<|0.5|	~54	<|0.5|	N/A^e	+30 (blue)^d
2-CF$_2$H + DMF → [**2-CF$_2$H**···DMF]	−5.5	4.93	1424.5	−4.97	−250	+36 (blue)
2-OH + DMF → [**2-OH**···DMF]	−11.2	1.42	1546.6	−1.51	−32	−350 (red)
2 H$_2$O → (H$_2$O)$_2$	−5.2	0.69	577.5	−0.95	−6.3	−64 (red)^d
G + C → GC base pair	−27.7	3.42	2021.8	−3.63	−35	−273 (red)^d

^{a}From left to right: bond energy, E, change in the average binding energy (= electronegativity equalization), $\Delta\bar{\chi}$, nuclear-repulsion, V_{NN}/n, and multielectron-contribution per electron summed with nuclear repulsion, $(V_{NN}+\omega)/n$, for selected intra- and intermodular interactions. All energies in kcal/mol. Two decimal places are given for $\Delta\bar{\chi}$ and $(V_{NN}+\omega)/n$ so that Q can be calculated.

^{b}Q descriptor (unitless) separates interactions governed by orbital stabilization (Q>0) from interactions governed by charge transfer (Q<0).

^{c}Frequency shift of hydrogen bond donor X–H bond stretch calculated at the M06-2X/6-31+G(d,p) level (cm^{-1}, unscaled).

^{d}Average shift of symmetric and asymmetric X–H bond stretches in hydrogen bond acceptor.

$^e\Delta\bar{\chi}$ for (CH2F2)2 –formation is small and its sign depends on the geometry, in turn sensitive to the level of theory. Q cannot be safely assigned.